Available online at www.sciencedirect.com
SCIENCE DIRECT®
Pergamon
Cement and Concrete Research 34 (2004) 1331–1339
CEMENT AND CONCRETE RESEARCH

Modeling bond strength of corroded reinforcement without stirrups

Xiaohui Wang*, Xila Liu

Department of Civil Engineering, Shanghai Jiaotong University, Minhang, Shanghai 200240, PR China

Received 20 August 2003; accepted 16 December 2003

Abstract

Deterioration of bond strength between concrete and reinforcement is of great importance in studying the strength of structural members with corroded reinforcements. A simple analytical model is proposed to demonstrate the effect of corrosion of reinforcing bar on reduction of bond strength. The corrosion pressure due to expansive action of corrosion products before and after corrosion cracking is firstly estimated. Then, reduction of bar confinement caused by cover cracking, change of friction coefficient between the steel and the concrete, and reduction of the friction force on the bearing face as well as deterioration of the ribs of the deformed bars due to steel corrosion are considered in calculating the mechanical interactions between reinforcing bar and concrete. As a result, the bond strength of corroded bars is calculated. The theoretical results are compared with the experimental results and agree with those results well.

Keywords: Bond strength; Corrosion; Concrete; Friction

1. Introduction

Corrosion of reinforcing bar can greatly influence the bond strength between deformed bars and concrete. First, the accumulated corrosion products on the bar surface cause longitudinal cracking of the concrete cover. Loss of concrete cover implies loss of confinement and a reduction in bond strength at the interfacial zone between the two materials. Second, the soft layer created by the accumulated corrosion products on the bar surface may effectively reduce the friction component of the bond strength. In addition, the deterioration of the ribs of the deformed bars causes a significant reduction of the interlocking forces between the ribs of the bars and the surrounding concrete keys. This deteriorates the primary mechanism of the bond strength between deformed bars and concrete, and hence, the bond strength decreases significantly.

Many research works [1–9] have been carried out to study the bond behavior of corroded reinforcements. However, these works are experimental. The empirical formulae that describe what influence corrosion has on the bond strength are based on the corresponding test results. However, it is difficult to determine how the bond mechanism is affected by reinforcement corrosion from these empirical formulae because of the high dependence upon corresponding experimental details. Recently, general models for prediction of bond strength of corroded bars are proposed [10–12]. Three-dimensional finite element program DIANA was used to model the effect of corrosion on bond strength [10]; a model to predict both the pressure around a corroded bar and the bond strength at the onset of pullout in an anchorage was proposed [11]. However, the residual confinement pressure given by the cracked concrete around the bar is measured from the tests of Baldwin and Clark [11] after the splitting strength of concrete cover, not obtained by theoretical modeling. Bond strength for corroded bars before and after corrosion cracking is theoretically modeled [12]. For a larger ratio of cover-to-bar diameter, when the smeared hoop strain at the inner boundary of the thick-walled cylinder reaches the maximum cracking strain of concrete in tension, the redistribution of the radial displacement for cover concrete is not considered. Meanwhile, the influence of steel corrosion on the friction force on the bearing face is not considered in calculating the interactions between the corroded bar and concrete.

In the present paper, basing on the methodology proposed by Wang and Liu [12], bond strength of corroded reinforcements in reinforced concrete specimens without stirrups is calculated. Corrosion pressure prior to the

* Corresponding author.
E-mail address: w_xiaoh@163.com (X. Wang).

0008-8846/$ – see front matter © 2004 Elsevier Ltd. All rights reserved.
doi:10.1016/j.cemconres.2003.12.028

loading of the reinforcing bar and to the development of bond is modeled firstly [11–12]. The redistribution of the radial displacement for cover concrete is considered after the smeared hoop strain at the inner boundary of the thick-walled cylinder reaches the maximum cracking strain of concrete in tension. The influence of steel corrosion on the friction force on the bearing face is considered in calculating the interactions between the corroded bar and concrete. Then, bond strength of corroded reinforcements is calculated by considering the additional contribution of corrosion pressure. The comparison of the modeling results and the test results shows that the model is practicable in predicting the bond strength of corroded reinforcements.

2. Corrosion pressure

2.1. Corrosion pressure before corrosion cracking ($x \le x_{cr}$)

The methodology proposed by Wang and Liu [12] is used to evaluate the corrosion pressure caused by the corrosion of reinforcing bar. The problem is modeled with reference to Fig. 1, wherein the reinforcing bar of initial radius R_0 is embedded in concrete with R_c, which is the cover dimension. $R_c = R_0 + c$, where c is the lowest thickness of horizontal and vertical concrete cover. Smeared cracking is assumed; therefore, the formulation is written in terms of average stresses and strains [13]. At the distance $r = R_i$, the cracking strain limit of the concrete in tension ε_{ct} has been reached. $\varepsilon_{ct} = f_t/E_0$, where f_t is the tensile strength of concrete and E_0 is the initial elastic modulus of concrete. Influence of reinforcement corrosion on f_t and E_0 is neglected. R_i defines the crack front.

Assuming uniform corrosion on the bar surface, the attack penetration depth or radius loss of the bar is defined as x. Then, the reduced radius of bar R_s is given by $R_s = R_0 - x$. The corresponding volume of the steel consumed per unit length of the bar is given by $\Delta V_s = \pi R_0^2 - \pi R_s^2 = 2\pi R_0 x - \pi x^2$. And the corresponding volume of accumulated rust products on the bar perimeter is $\Delta V_r = n \cdot \Delta V_s$, where n is the ratio between the volume of rust products and virgin steel, and the value of n is taken as approximately 1.7–6.15, according to different corrosion products [10].

Considering that a fraction of corrosion products propagate away from the bar surface through the cracks and pores of concrete toward the free surface, the volume of accumulated rust products is [13]

$$\Delta V_r = n \cdot \Delta V_s = \pi \cdot t_r (2R_s + t_r) + \sum w \cdot (R_i - R_r)/2.0 \tag{1}$$

where Σw is the total amount of crack width openings around the perimeter of the rust front R_r, given by $\Sigma w = 2\pi \cdot u_r|_{r=R_0} = 2\pi \cdot (R_r - R_0)$. $R_r = R_s + t_r$, where t_r, is the thickness of rust layer [12]:

$$t_r = \frac{n(2R_0 x - x^2) + x \cdot (R_i - R_0 + x)}{R_i + R_0} \tag{2}$$

The radial displacement $u_r|_{r=R_0}$ (Fig. 1b) caused by corrosion pressure is [12]

$$u_r|_{r=R_0} = R_r - R_0 = t_r - x = \frac{(n-1) \cdot (2R_0 x - x^2)}{R_i + R_0} \tag{3}$$

And the corresponding smeared hoop strain $\varepsilon_\theta|_{r=R_0}$ is $\varepsilon_\theta|_{r=R_0} = u_r|_{r=R_0}/R_0$.

Now, consider an equivalent corrosion pressure p_{cor} of the radial displacement $u_r|_{r=R_0}$ (Fig. 1c). Under the action of this equivalent corrosion pressure p_{cor}, the hoop stresses of the thick-walled cylinder reach the tensile strength of concrete f_t at $r = R_i$. Cracking in concrete in the inner part of the thick-walled cylinder is modeled as a process of softening that begins with the exceeding of the tensile strain capacity of concrete at a smeared hoop strain $\varepsilon_\theta(r) > \varepsilon_{ct}$ and is concluded at a smeared hoop strain $\varepsilon_\theta(r) = \varepsilon_u$, where ε_u corresponds to zero residual tensile strength (Fig. 2).

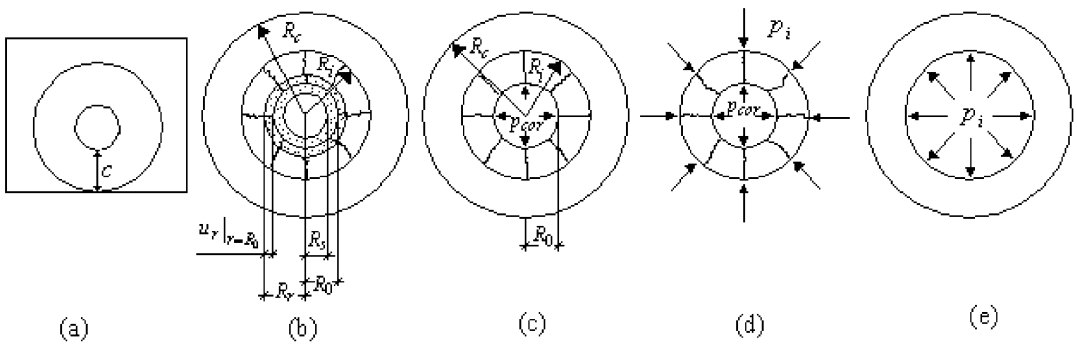

Fig. 1. (a) Cylinder model; (b) A thick-walled cylinder undergoes a radial displacement $u_r|_{r=R_0}$ at the inner boundary; (c) A thick-walled cylinder undergoes an equivalent pressure p_{cor} of $u_r|_{r=R_0}$ at the inner boundary; (d) The cracked inner part; (e) The elastic outer part.

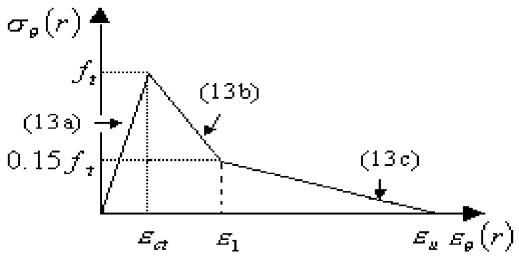

Fig. 2. Average stress–strain relationship of concrete in tension [13].

Consider the case of $\varepsilon_\theta|_{r=R_0} \le \varepsilon_u$, the linear-elastic displacement filed is assumed, and the distribution of the radial displacement for the whole concrete cover ($R_0 \le r \le R_c$) is given by [14]

$$u(r) = \frac{f_t}{E_0} \cdot r \cdot \frac{(R_c/r)^2 + 1}{(R_c/R_i)^2 + 1} \tag{4}$$

Then the radial displacement at $r = R_0$ is given as the following [12]:

$$u(r = R_0) = \frac{f_t}{E_0} \cdot R_0 \cdot \frac{(R_c/R_0)^2 + 1}{(R_c/R_i)^2 + 1} \tag{5}$$

Equating Eq. (3) to Eq. (5), the following equation is given [12]:

$$\frac{(n-1) \cdot (2R_0 x - x^2)}{R_i + R_0} = \frac{f_t}{E_0} \cdot R_0 \cdot \frac{(R_c/R_0)^2 + 1}{(R_c/R_i)^2 + 1} \tag{6}$$

Considering that $R_0 \le R_i \le R_c$, the value of different attack penetration depth x can be obtained by Eq. (6) at a different value of crack front R_i.

In the case of $\varepsilon_\theta|_{r=R_0} > \varepsilon_u$, variable RRu is introduced, where RRu is defined as $\mathrm{RRu} = u_r|_{r=R_0}/\varepsilon_u$. Basing on the assumption of the linear-elastic displacement filed, the distribution of the radial displacement for the concrete cover $\mathrm{RRu} \le r \le R_c$ is also given by Eq. (4). If a constant distribution of the radial displacement for the concrete cover $R_0 \le r \le \mathrm{RRu}$ is assumed [15], then the radial displacement at $r = R_0$ is equal to the radial displacement at $r = \mathrm{RRu}$ and given as the following:

$$u(r = R_0) = u(r = \mathrm{RRu}) = \frac{f_t}{E_0} \cdot \mathrm{RRu} \cdot \frac{(R_c/\mathrm{RRu})^2 + 1}{(R_c/R_i)^2 + 1} \tag{7}$$

Equating Eq. (3) to Eq. (7), the following equation is given:

$$\frac{(n-1) \cdot (2R_0 x - x^2)}{R_i + R_0} = \frac{f_t}{E_0} \cdot RRu \cdot \frac{(R_c/\mathrm{RRu})^2 + 1}{(R_c/R_i)^2 + 1} \tag{8}$$

Considering that $\mathrm{RRu} \le R_i \le R_c$, the value of different attack penetration depth x can be obtained by the iterating solution of Eq. (8) and $\mathrm{RRu} = u_r|_{r=R_0}/\varepsilon_u$ at a different value of crack front R_i.

When the crack front R_i in Eqs. (6) or (8) reaches the external radius R_c, the corresponding attack penetration depth is defined as the critical attack penetration depth x_{cr} of the reinforcing bar.

To obtain the corrosion pressure p_{cor} in Fig. 1d, considering the equilibrium conditions written along any radially cracked section, the following equation can be given [12]:

$$p_{cor} \cdot R_0 = p_i \cdot R_i + \int_{R_0}^{R_i} \sigma_\theta(r) dr \tag{9}$$

where p_i can be obtained by setting $\sigma_\theta(r = R_i) = f_t$ of the elastic outer part (Fig. 1e)

$$p_i = f_t \cdot \frac{R_c^2 - R_i^2}{R_c^2 + R_i^2} \tag{10}$$

To estimate $\sigma_\theta(r)$ in the cracked inner part (see Fig. 1d), the hoop stress and the corresponding radial displacement distribution in this inner ring are considered. First, the total extension of a circumferential fiber at a distance r is given by [12]

$$2\pi \cdot r\varepsilon_\theta(r) = 2\pi \cdot u(r) \tag{11}$$

Then, the hoop strain $\varepsilon_\theta(r)$ at position r can be given as [12]

$$\varepsilon_\theta(r) = \frac{u(r)}{r} = \frac{f_t}{E_0} \cdot \frac{(R_c/r)^2 + 1}{(R_c/R_i)^2 + 1} \tag{12}$$

It is evident that $\varepsilon_\theta(r) \ge f_t/E_0 = \varepsilon_{ct}$. The following equations that describe the relationship between average hoop stress $\sigma_\theta(r)$ and strain $\varepsilon_\theta(r)$ of concrete in tension are used (see Fig. 2) [13]:

$$\sigma_\theta(r) = E_0 \cdot \varepsilon_\theta(r) \qquad \varepsilon_\theta(r) \le \varepsilon_{ct} \tag{13a}$$

$$\sigma_\theta(r) = f_t \cdot \left[1 - 0.85 \cdot \frac{\varepsilon_\theta(r) - \varepsilon_{ct}}{\varepsilon_1 - \varepsilon_{ct}}\right] \qquad \varepsilon_{ct} < \varepsilon_\theta(r) \le \varepsilon_1 \tag{13b}$$

$$\sigma_\theta(r) = 0.15 f_t \frac{\varepsilon_u - \varepsilon_\theta(r)}{\varepsilon_u - \varepsilon_1} \qquad \varepsilon_1 < \varepsilon_\theta(r) \le \varepsilon_u \tag{13c}$$

where the relationship between $\sigma_\theta(r)$ and $\varepsilon_\theta(r)$ is assumed to be linear-elastic prior to cracking, with a slope equal to E_0; the values of ε_1 and ε_u in Fig. 2 are taken as $\varepsilon_1 = 0.0003$ and $\varepsilon_u = 0.002$, respectively [13].

To calculate the integral $\int_{R_0}^{R_i} \sigma_\theta(r) dr$ in Eq. (9), the variable RR1 is defined according to Eq. (12):

$$\mathrm{RR1} = \frac{R_c}{\sqrt{\varepsilon_1 \cdot E_0/f_t \cdot [(R_c/R_i)^2 + 1] - 1}} \tag{14}$$

Where RR1 is the radial distance in which the hoop strains reach ε_1. Considering the relationship between R_0 and RR1 RRu, the integral $\int_{R_0}^{R_i} \sigma_\theta(r) dr$ can be calculated. And the corresponding corrosion pressure p_{cor} at a different attack

penetration depth x ($x \le x_{cr}$) of the reinforcing bar can be obtained.

2.2. Corrosion pressure after corrosion cracking($x > x_{cr}$)

Taking $R_i = R_c$ into Eq. (3), the radial displacement at $r = R_0$ can be given as the following when corrosion level $x > x_{cr}$ [12]:

$$u_r|_{r=R_0} = \frac{(n-1)\cdot(2R_0x - x^2)}{R_c + R_0} \tag{15}$$

Similar to the equilibrium condition of Eq. (9), the following equilibrium equation is given to obtain the corrosion pressure p_{cor} after corrosion cracking [12]:

$$p_{cor}\cdot R_0 = \int_{R_0}^{R_c} \sigma_\theta(r)dr \tag{16}$$

To estimate $\sigma_\theta(r)$ in Eq. (16), the radial displacement distribution in the whole cracked range $R_0 \le r \le R_c$ is considered. The radial displacement distribution in the whole cracked range $R_0 \le r \le R_c$ can be assumed as the following [12]:

$$u(r) = \varepsilon_{\theta c}\cdot r \cdot \frac{(R_c/r)^2 + 1}{2} \tag{17}$$

where $\varepsilon_{\theta c}$ is the hoop strain at R_c. And the corresponding hoop strain $\varepsilon_\theta(r)$ at position r can be given as the following, according to Eq. (11) [12]:

$$\varepsilon_\theta(r) = \frac{u(r)}{r} = \varepsilon_{\theta c}\cdot\frac{(R_c/r)^2 + 1}{2} \tag{18}$$

where the range of $\varepsilon_\theta(r)$ is $\varepsilon_{ct} < \varepsilon_\theta(r) \le \varepsilon_u$.

In the case of $\varepsilon_\theta|_{r=R_0} \le \varepsilon_u$, the unknown hoop strain $\varepsilon_{\theta c}$ can be obtained by equating Eq. (15) to $u(r = R_0)$ of Eq. (17) [12]:

$$\frac{(n-1)\cdot(2R_0x - x^2)}{R_c + R_0} = \varepsilon_{\theta c}\cdot R_0 \cdot \frac{(R_c/R_0)^2 + 1}{2} \tag{19}$$

While for the case of $\varepsilon_\theta|_{r=R_0} > \varepsilon_u$, RRu is still defined as $\mathrm{RRu} = u_r|_{r=R_0}/\varepsilon_u$. On the base of the assumption of the equal radial displacement at $r = R_0$ and $r = \mathrm{RRu}$, the unknown hoop strain $\varepsilon_{\theta c}$ can be obtained from Eq. (20)

$$\frac{(n-1)\cdot(2R_0x - x^2)}{R_c + R_0} = \varepsilon_{\theta c}\cdot \mathrm{RRu}\cdot\frac{(R_c/\mathrm{RRu})^2 + 1}{2} \tag{20}$$

Using the relationship between $\sigma_\theta(r)$ and $\varepsilon_\theta(r)$ of Eqs. (13a), (13b), and (13c) and defining the variable $\mathrm{RR1} = R_c/\sqrt{(2\varepsilon_1)/\varepsilon_{hc} - 1}$ according to Eq. (19), the integral $\int_{R_0}^{R_c}\sigma_\theta(r)dr$ in Eq. (16) can be calculated. And the corrosion pressure p_{cor} at different attack penetration depth x after corrosion cracking ($x > x_{cr}$) can be obtained.

3. Bond strength model

The methodology proposed by Xu [16] is adopted to calculate the bursting and friction forces produced by the bond action of ribbed bars. The geometry of a ribbed bar and the mechanical interactions between the bar and concrete under splitting failure can be seen in Fig. 3a [16], where the rib face angle $\varphi = 45°$; the core diameter d_0 is

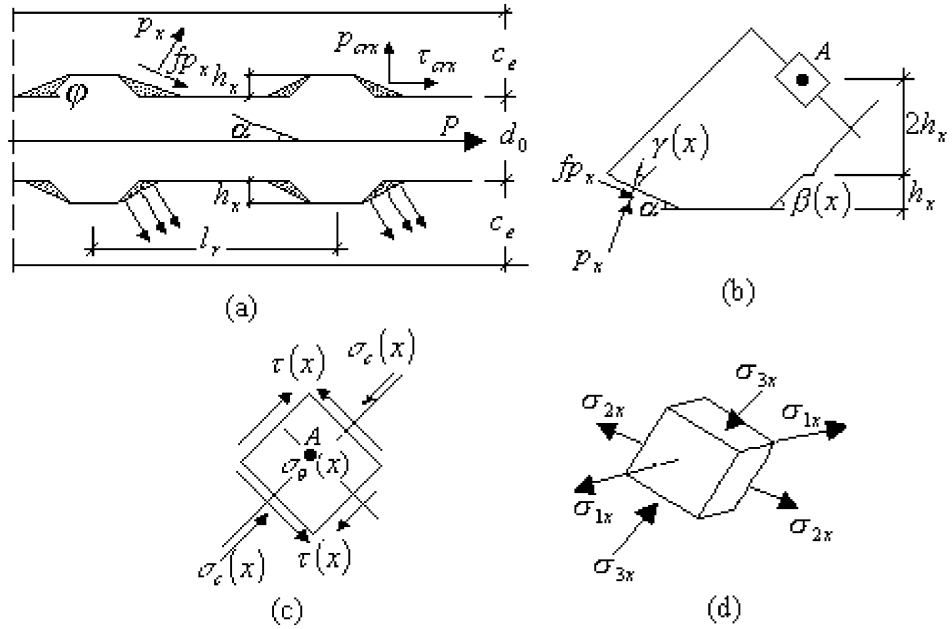

Fig. 3. (a) Geometry of a ribbed bar and the mechanical interaction between bar and concrete; (b) Point A at the end of concrete key; (c) Stresses of Point A; (d) Principal stresses of Point A [16].

taken as $d_0 = 0.96d$, where d is the nominal diameter of the noncorroded reinforcing bar; the rib spacing l_r is taken as $l_r = 0.6d$. When the attack penetration depth reaches x, the nominal diameter d_x of the corroded reinforcing bar is $d_x = d - 2x$. According to Xu [16], the average rib height of noncorroded bar is $0.07d$; then, the average rib height h_x in Fig. 3a at corrosion level x can be approximately taken as $0.07d_x$. α is the angle of the face of crushed concrete. The average value of α is taken as $\alpha = 25°$. As for the mechanical interactions between the bar and concrete, p_x and fp_x are the normal compressive force and friction force of the bearing face; where f is the friction coefficient of crushed concrete, p_{crx} is the average radial force, and τ_{crx} is the splitting bond anchorage strength.

For noncorroded reinforcing bar, the angle of the inclination of the inclined cracking β is [16]

$$\beta = \frac{1}{2}\arctan\left[-\frac{2(\sin\varphi + \mu\cos\varphi)}{\cos\varphi - \mu\sin\varphi}\right] + 90^\circ \tag{21}$$

where μ is the friction coefficient between noncorroded reinforcement and concrete, μ=0.3. For friction coefficient between corroded reinforcing bar and concrete, the following formulation is adopted to consider the influence of accumulated corrosion products on the bar surface [11]:

$$\mu = \mu(x) = 0.37 - 0.26 \cdot (x - x_{cr}) \tag{22}$$

Taking Eq. (22) into Eq. (21), and $\beta = \beta(x)$ at different corrosion levels x can be obtained. The angle between the direction of p_x and the inclined cracking can be given as $\gamma(x) = 90° - \alpha - \beta(x)$[12].

For noncorroded reinforcing bar, the suggested value of f under splitting failure (Fig. 3a) is $f = 0.6$ [16]. While for corroded reinforcing bar, due to the accumulation of corrosion products at the steel–concrete surface, the friction coefficient of crushed concrete f is greatly influenced. Assuming f decreases with the increasing of thickness of the rust layer t_r, the following formulation is suggested to consider the effect of accumulation of corrosion products on f:

$$f = f(x) = 0.6 \cdot \left(1.0 - \frac{t_r}{h_x}\right) \tag{23}$$

where t_r is given by Eq. (2) before corrosion cracking ($x \le x_{cr}$); when $x > x_{cr}$, $t_r = [n(2R_0x - x^2) + x\cdot(R_c - R_0 + x)]/(R_c + R_0)$. f is assumed to be zero if the rust layer t_r reaches the average rib height h_x of corroded bars; if $t_r > h_x$, $f = 0.0$.

Then, on the basis of two assumptions, (1) two times of the average rib height of the extended length of the inclined cracking, and (2) uniform stress distribution at the end of the concrete key [16], the stresses of point A in Fig. 3b,c is given as the following by considering the reduction of the friction force on the bearing face fp_x, which is described in Eq. (23):

$$\sigma_c(x) = [\cos\gamma(x) + f(x)\cdot\sin\gamma(x)] \cdot p_x \cdot \frac{\pi\cdot(d_0 + h_x)\cdot h_x/\sin\alpha}{\pi\cdot(d_0 + 6h_x)\cdot l_r\cdot\sin\beta(x)} \tag{24}$$

$$\tau(x) = [-\sin\gamma(x) + f(x)\cdot\cos\gamma(x)] \cdot p_x \cdot \frac{\pi\cdot(d_0 + h_x)\cdot h_x/\sin\alpha}{\pi\cdot(d_0 + 6h_x)\cdot l_r\cdot\sin\beta(x)} \tag{25}$$

And the average radial pressure p_{crx} is given as following:

$$p_{crx} = [\cos\alpha - f(x)\cdot\sin\alpha]\cdot p_x \cdot \frac{\pi\cdot(d_0 + h_x)\cdot h_x/\sin\alpha}{\pi\cdot d_x\cdot l_r} \tag{26}$$

Basing on the assumption of the trapezoid distribution of hoop stress along the concrete cover, as well as maximum stress at the inner surface $d_x/2$ and zero stress at the critical

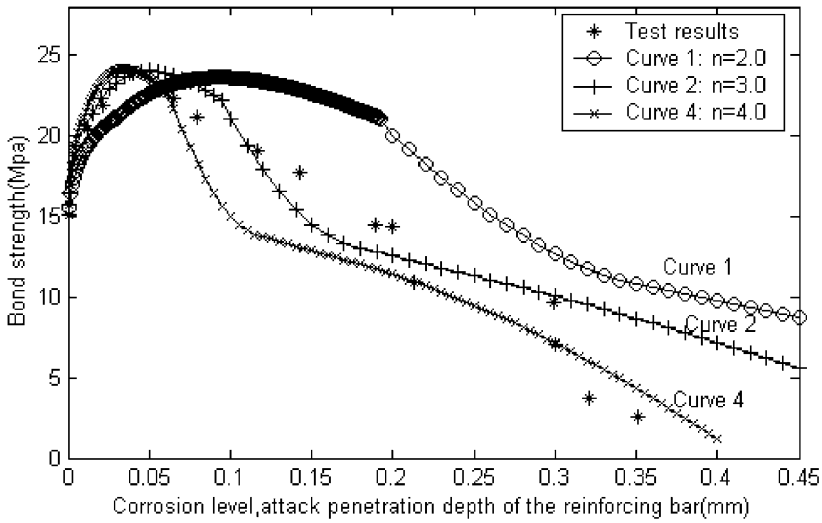

Fig. 4. Bond strength versus corrosion levels: specimens with 10-mm deformed bars [1].

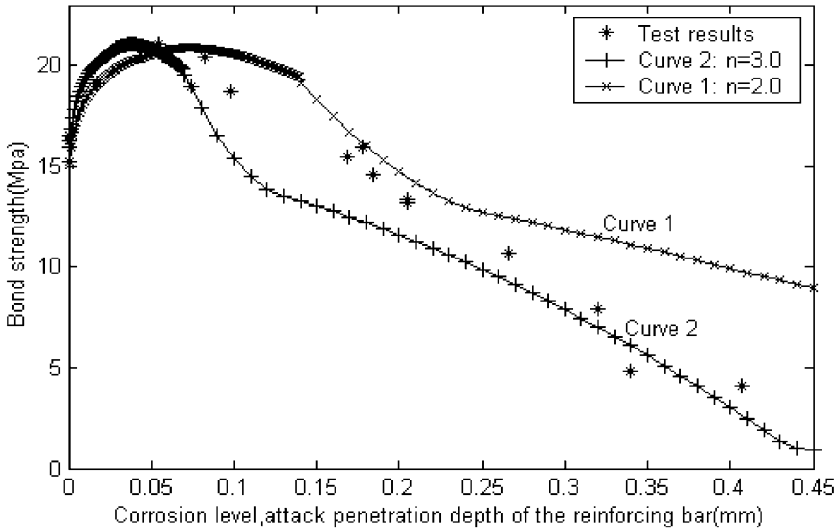

Fig. 5. Bond strength versus corrosion levels: specimens with 14-mm deformed bars [1].

cover/diameter = 4.5 [16], the hoop tensile stress $\sigma_\theta(x)$ under p_{crx} is

$$\sigma_\theta(x) = \frac{10}{9}\left(1 - \frac{3h_x + d_0/2}{5d_x}\right) \cdot \frac{1}{2 \cdot (1 - \frac{c_e}{9d_x}) \cdot c_e/d_x} \cdot p_{crx} \tag{27}$$

where c_e is effective depth of concrete cover of corroded bar and is defined as

$$\mathrm{RRu} \le R_0 \quad c_e = R_c - R_0 = c \tag{28a}$$

$$R_0 < \mathrm{RRu} < R_c \quad c_e = R_c - \mathrm{RRu} \ge 3h_x \tag{28b}$$

If $c_e < 3h_x$, c_e is taken as $c_e = 3h_x$.

Then, the principal stresses and the corresponding three stress invariants can be obtained by theory of elasticity–plasticity [16]. The failure criterion of Ottosen [17] is used to calculate the failure condition of concrete under multiaxial stress state, and the unknown normal compressive force p_x can be obtained. Therefore, splitting bond strength τ_{crx} can be given as

$$\tau_{crx} = [\sin\alpha + f(x) \cdot \cos\alpha] \cdot p_x \cdot \frac{\pi \cdot (d_0 + h_x) \cdot h_x}{\pi \cdot l_r \cdot d_x \cdot \sin\alpha} \tag{29}$$

Considering the corrosion pressure p_{cor} prior to the loading and assuming that the direction of p_{cor} is the same

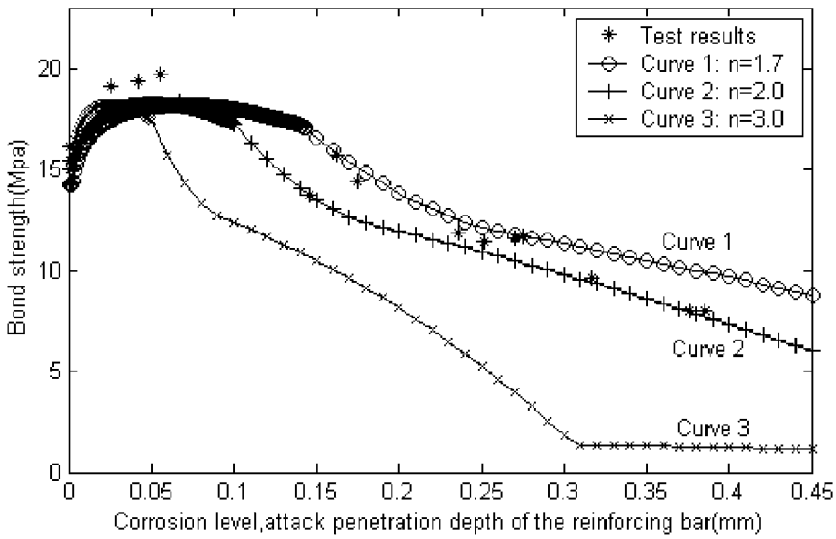

Fig. 6. Bond strength versus corrosion levels: specimens with 20-mm deformed bars [1].

Table 1
Comparison with the calculated and experimental attack penetration depth

c (mm)	d (mm)	Test x_{cr} (mm)	Calculated x_{cr} (mm)			
			$n=1.7$	$n=2.0$	$n=3.0$	$n=4.0$
70	10	Approximately 0.143–0.377	0.277	0.192	0.095	0.063
68	14	Approximately 0.098–0.169		0.139	0.069	
65	20	Approximately 0.100–0.146	0.144	0.100	0.050	

as that of p_{crx}, the ultimate bond strength of corroded reinforcements under splitting failure can be formulated as the following [12]:

$$\tau_{cr}(x) = \tau_{crx} + \tan\alpha \cdot p_{cor} \tag{30}$$

4. Comparison with test results

4.1. Comparison with test results of Al-Sulaimani et al. [1]

Pullout test was conducted on 150-mm cubic concrete specimens with 10-, 14-, and 20-mm-diameter deformed bars embedded centrally. The concrete had an average compressive strength of 30 MPa. Corrosion is measured as the loss of metal relative to the original bar weight. The attack penetration depth of the test results is estimated as follows. First, basing on the data of Table 4 of Ref. [1], the relationship between the corrosion mass loss percent p_{mass} (%) and the reduction in steel area percent p_{area} (%) can be linearly regressed as $p_{area}=a+b\cdot p_{mass}$, where a and b are linear regression coefficients: $a=-0.04867$, $b=2.47858$. Then, the attack penetration depth x of reinforcing bar is $x=(1-\sqrt{1-0.01\cdot p_{area}})\cdot d/2(\text{mm})$. Second, Faraday's law is used, and the attack penetration depth x is determined by [7] $x=p_{mass}\cdot d/400$ (mm). The actual attack penetration depth is taken as follows: $x_{test}=0.5[(1-\sqrt{1-0.01\cdot p_{area}})\cdot d/2+p_{mass}\cdot d/400]$.

The calculated results are compared with the test results (see Figs. 4, 5, and 6 for specimens with 10-, 14-, and 20-mm-diameter deformed bars, respectively). It can be seen that the calculated bond strength agrees well with the results of experimental study. The calculated critical attack penetration depth of reinforcing bars is compared with the experimental results (see Table 1).

4.2. Comparison with the test results of Cabrera and Ghoddoussi [2]

Pullout tests were carried out on 150-mm concrete cubes with a 12-mm-diameter reinforcing bar centrally embedded in the cube. The average 28-day compressive strength of the opc mix was 56 MPa. The amount of corrosion on the steel of the pullout specimens was found by the gravimetric weight–loss method. Due to the relative agreement between measured reinforcement weight loss and calculated reinforcement weight loss by Faraday's law [18], the attack penetration depth x is determined by $x=p_{mass}\cdot d/400$ (mm), where p_{mass} is the weight or mass loss percent.

Bond strength at different levels of corrosion is calculated and compared with the test results (see Fig. 7). It is seen from Fig. 7 that the test results fall in between the calculated bond strength in the cases of $n=2.0$ and $n=3.0$. The calculated critical attack penetration depth of reinforcing bar is $x_{cr}=0.148$ mm in the case of $n=20$ and $x_{cr}=0.073$ mm in the case of $n=3.0$; while the experimental critical attack penetration depth of reinforcing bar is $x_{cr}=0.067$ mm.

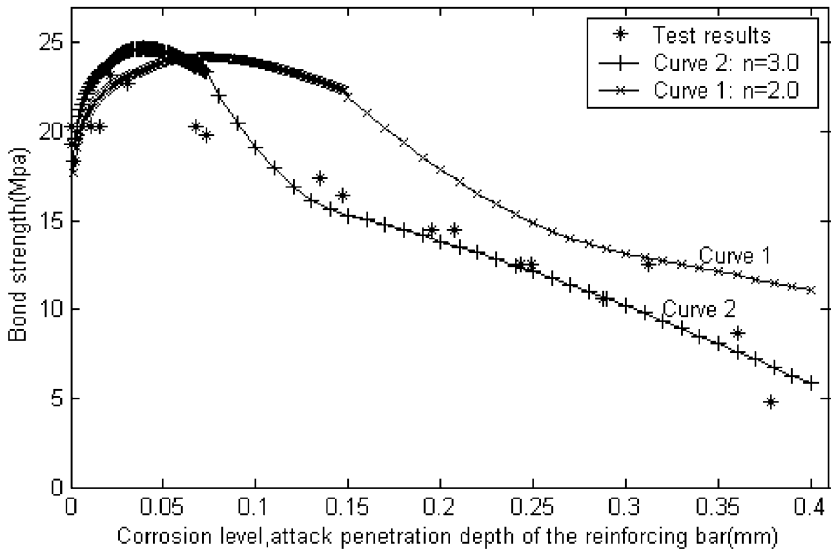

Fig. 7. Bond strength versus corrosion levels: specimens with 12-mm deformed bars [2].

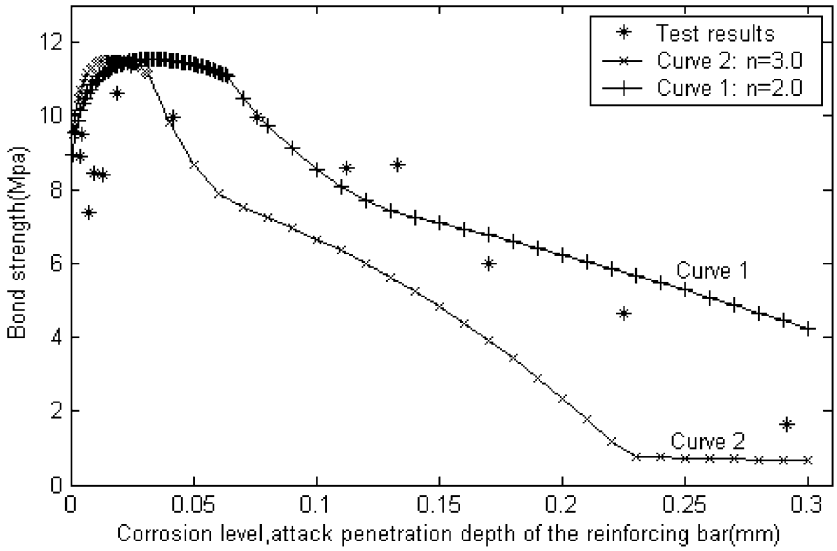

Fig. 8. Bond strength versus corrosion levels: specimens with 12-mm deformed bars [9].

4.3. Comparison with test results of Zhao and Jin [9]

A pullout test was conducted on 100-mm cubic concrete specimen with a 12-mm-diameter deformed bar embedded centrally. The average compressive strength of the concrete cubes after 28 days was 22.13 MPa. Corrosion was determined by applying Faraday's law.

Bond strength at different levels of corrosion is calculated and compared with the test results (see Fig. 8). It is seen from Fig. 8 that the experimental results fall in between the calculated bond strength in the cases of $n=2.0$ and $n=3$. The maximum bond strength of test results occurs at the corrosion level $x=0.0243$ mm; while the calculated ones are given at $x=0.033$ mm in the case of $n=2.0$ and $x=0.017$ mm in the case of $n=3$.

5. Conclusions

In the present paper, basing on the methodology proposed by Wang and Liu [12], the bond strength of corroded reinforcements in reinforced concrete specimens without stirrups is calculated. Corrosion pressure prior to the loading of the reinforcing bar and to the development of bond is modeled firstly by consideration of the distribution of the radial displacement for the concrete cover and the softening behaviour of the cracked concrete. When the smeared hoop strain at the inner boundary of the thick-walled cylinder reaches the maximum cracking strain of concrete in tension ε_u, the redistribution of the radial displacement for cover concrete is considered. Then, to consider the reduction of the friction force on the bearing face fp_x due to the accumulation of corrosion products among the spacing of the ribs of the deformed reinforcing bar, Eq. (23) is proposed. Then, the interactions between the corroded bar and concrete are calculated by using the methodology proposed by Xu [16]. As a result, the bond strength of corroded reinforcements is calculated by considering the additional contribution of corrosion pressure. The comparison of the modeling results and the test results shows that the model is practicable in predicting the bond strength of corroded reinforcements.

The calculated critical attack penetration depth x_{cr} is compared with the corresponding values of the experimental results. The calculated x_{cr} is mainly dependent on the cover depth, diameter of reinforcing bar, tensile strength of concrete, elastic modulus of concrete, and the volume ratio between rust and uncorroded steel.

The bond strength of corroded deformed bars depends mainly on the interlocking forces between the ribs of the bars and the surrounding concrete. Whether or not the concrete cover is cracked by corrosion pressure prior to the loading of the bars does not influence this dominant mechanism of bond strength. Bond strength of corroded bars remains available as long as the confinement around the bar is not completely impaired. When the concrete cover no longer provides confinement to the bars, bond strength is significantly reduced and becomes negligible.

It is seen from Figs. 4–8 that the calculated bond strength is greatly influenced by the volume ratio n between rust and uncorroded steel for a different ratio of clear cover-to-bar diameter. For a larger ratio of cover-to-bar diameter, such as the cover-to-bar diameter of 7.0 in Fig. 4, when a larger volume ratio n is selected, the calculated results agree with the test results better; while for an ordinary ratio of cover-to-bar diameter, such as the cover-to-bar diameter smaller than 5.0, values of volume ratio $n=2.0$ and $n=3.0$ are suitable. Therefore, further detailed research are needed to focus on the relationship between the choice of n and the ratio of clear cover-to-bar diameter in theoretical calculation. Meanwhile, the changes

of friction coefficient between corroded bars and concrete as well as friction coefficient of crushed concrete due to the accumulation of corrosion products still need more detailed research.

Acknowledgements

The authors gratefully acknowledge the support provided by the National Key Basic Research and Development Program (973 Program) No. 2002CB412709.

References

[1] G.J. Al-Sulaimani, M. Kaleemullah, I.A. Basunbul, Rasheeduzzafar, Influence of corrosion and cracking on bond behaviour and strength of reinforced concrete members, ACI Struct. J. 87 (2) (1990) 220–231.
[2] J.G. Cabrera, P. Ghoddoussi, The effect of reinforcement corrosion on the strength of the steel/concrete "bond", Proceedings of the International Conference on Bond in Concrete, Organized by CEB and Riga Technical University, Riga, Latvia, October 1992, pp. 10/11–10/24.
[3] A.A. Almusallam, A.S. Al-Gahtani, A.R. Aziz, Rasheeduzzafar, Effect of reinforcement corrosion on bond strength, Constr. Build. Mater. 10 (2) (1996) 123–129.
[4] X. Fu, D.L. Chung, Effect of corrosion on the bond between concrete and steel rebar, Cem. Concr. Res. 27 (12) (1997) 1811–1815.
[5] K. Stanish, R.D. Hooton, S.J. Pantazopoulou, Corrosion effects on bond strength in reinforced concrete, ACI Struct. J. 96 (6) (1999) 915–922.
[6] L. Amleh, S. Mirza, Corrosion influence on bond between steel and concrete, ACI Struct. J. 96 (3) (1999) 415–423.
[7] P.S. Mangat, M.S. Elgarf, Bond characteristics of corroding reinforcement in concrete beams, Mater. Struct. 32 (1999) 89–97.
[8] Y.B. Auyeung, P. Balaguru, L. Chung, Bond behavior of corroded reinforcement bars, ACI Mater. J. 97 (2) (2000) 214–221.
[9] Y.X. Zhao, W.L. Jin, Test study on bond behavior of corroded steel bars and concrete, J. Zhejiang University (Eng. Sci.) 36 (4) (2002) 352–356.
[10] K. Lundgren, Modelling the effect of corrosion on bond in reinforced concrete, Mag. Concr. Res. 54 (3) (2002) 165–173.
[11] D. Coronelli, Corrosion cracking and bond strength modeling for corroded bars in reinforced concrete, ACI Struct. J. 99 (3) (2002) 267–276.
[12] X.H. Wang, X.L. Liu, Modelling effects of corrosion on cover-cracking and bond in reinforced concrete, Mag. Concr. Res. (accepted for publication).
[13] S.J. Pantazopoulou, K.D. Papoulia, Modeling cover-cracking due to reinforcement corrosion in RC structures, J. Eng. Mech. 127 (4) (2001) 342–351.
[14] C.V. Nielsen, N. Bicanic, Radial fictitious cracking of thick-walled cylinder due to bar pull-out, Mag. Concr. Res. 54 (3) (2002) 215–221.
[15] H.W. Reinhardt, C. Van Der Veen, Splitting failure of a strain-softening material due to bond stresses, in: A. Carpinteri (Ed.), Applications of Fracture Mechanics to Reinforced Concrete, Elsevier, Amsterdam, The Netherlands, 1992, pp. 333–346.
[16] Y.L. Xu, Experimental study of anchorage properties for deformed bars in concrete, PhD thesis, Department of Civil Engineering, Tsinghua University, Beijing, April, 1990.
[17] N.S. Ottosen, A failure criterion for concrete, J. Eng. Mech. 103 (EM4) (1977) 527–535.
[18] J.G. Cabrera, Deterioration of concrete due to reinforcement steel corrosion, Cem. Concr. Compos. 18 (1996) 47–59.